Dysregulation of the microbiota-brain axis during long-term exposure to polystyrene nanoplastics in rats and the protective role of dihydrocaffeic acid

Wenbo Jiang, Cong Hu, Yunyan Chen, Yue Li, Xinyi Sun, Huanyu Wu, Ruiming Yang, Yiwei Tang, Fengru Niu, Wei Wei, Changhao Sun, Tianshu Han

PII: S0048-9697(23)00717-9

DOI: https://doi.org/10.1016/j.scitotenv.2023.162101

Reference: STOTEN 162101

To appear in: *Science of the Total Environment*

Received date: 9 September 2022

Revised date: 16 January 2023

Accepted date: 4 February 2023

Please cite this article as: W. Jiang, C. Hu, Y. Chen, et al., Dysregulation of the microbiota-brain axis during long-term exposure to polystyrene nanoplastics in rats and the protective role of dihydrocaffeic acid, *Science of the Total Environment* (2023), https://doi.org/10.1016/j.scitotenv.2023.162101

Dysregulation of the microbiota-brain axis during long-term exposure to polystyrene nanoplastics in rats and the protective role of dihydrocaffeic acid

Wenbo Jiang[1,2,3#], Cong Hu[1#], Yunyan Chen[1#], Yue Li[3], Xinyi Sun[1], Huanyu Wu[1], Ruiming Yang[1], Yiwei Tang[1], Fengru Niu[1], Wei Wei[1,4]*, Changhao Sun[1]*, Tianshu Han[1]*

[1]Department of Nutrition and Food Hygiene, the National Key Discipline, School of Public Health, Harbin Medical University, Harbin, P. R. China.

[2]Department of Toxicology, College of Public Health, Harbin Medical University, Harbin, Heilongjiang Province 150081, P. R. China.

[3]Department of Cardiology, the First Affiliated Hospital of Harbin Medical University, Harbin, China.

[4]Department of Pharmacology, College of Pharmacy Key Laboratory of Cardiovascular Research, Ministry of Education, Harbin Medical University, Harbin, P. R. China.

[#]Wenbo Jiang, Cong Hu and Yunyan Chen contributed equally.

[*]Correspondence to: Wei Wei, Changhao Sun and Tianshu Han, Department of Nutrition and Food Hygiene, 157 Baojian Road, Harbin, P. R. China 150081, Phone: 86-451-87502681, E-mail: weiweibubble1994@163.com; hmuchsun@163.com; snowcalendar@126.com.

Words: 5123

Numbers of Tables and Figures: 6

ABSTRACT

Polystyrene nano-plastics (PS-NPs) can be accumulated in the food chain and can penetrate biological barriers to affect multiple physiological functions. However, the adverse effects of nano-plastics on mammals and the underlying mechanism still remain unknown. To fill the gaps, our study administrated low-dose PS-NPs (50 and 100 μg/L) for 24 consecutive weeks in rats. Behavioral and morphological evaluations were performed to assess the neurobehavoirs. A combined analysis of multiple omics was used to evaluate the dysfunctions of the gut-microbe-brain axis. After dihydrochalcone(NHDC) treatment in the PS-NPs rat model, the inflammation response and apoptosis process were assessed and proteomics was used to explore the underlying mechanism. Our results indicated that long-term exposure to low-dose PS-NPs could induce abnormal neurobehaviors and amygdaloid nucleus impairment, and stimulate inflammatory responses and apoptosis. Metagenomics results revealed that four microbial phyla including *Proteobacteria*, *Firmicutes*, *Defferibacteres*, and *Bacteroidetes* changed significantly compared to the control. Targeted metabolomics analysis in the feces showed alteration of 122 metabolites induced by the PS-NPs exposure, among which the content of dihydrocaffeic acid was significantly associated with the different microbial genera and pivotal differential metabolites in the amygdaloid nucleus. And NHDC treatment significantly alleviated PS-NP-induced neuroinflammation and apoptosis and the cyclic adenosine monophosphate(cAMP)/protein kinase A(PKA)/phosphorylated cAMP-response element binding protein(p-CREB)/plasma membrane calcium-transporting ATPase

2(Atp2b2) signaling pathway was identified in the proteomics. In conclusion, long-term exposure to low-dose PS-NPs has adverse effects on emotion through the dysregulation of the gut-brain axis, and dihydrocaffeic acid can alleviate these effects via the cAMP/PKA/p-CREB/Atp2b2 signaling pathway.

KEYWORDS: Nano-plastics; Long-term exposure; Anxiety-like behavior; Microbiota-brain axis; Muti-omics

INTRODUCTION

Recently, much attention has been placed on the migration, transformation and health impacts of plastic particles, especially for the nanoplastics (NPs), in the environment. NPs are plastic fragments or particles with a size <1 μm^3 that exhibit physical and chemical properties different from those of bulk materials. A few experimental studies have found that various plastic food packages, such as coffee cup lids, plastic tea bags, can degrade into NPs (Lambert and Wagner, 2016; Hernandez et al., 2019). Furthermore, accumulating evidence has indicated that NPs can be inhaled or ingested with drinks and food (Jiang et al., 2020; Banerjee A et al., 2021), and the smaller plastic particles are more easily internalized into organisms (Stock et al., 2021). More importantly, a recent study detected the NPs in human's intestinal and liver cells, which either attached directly to the membrane or were trapped in membrane vesicles (Lu et al., 2022). Therefore,elucidating the potential health impacts of NP exposure is an important endeavor.

Existing studies have shown that dorganisms are mainly exposed to NPs through the digestive tract (Rodrigues et al., 2022; Hirt and Body-Malapel, 2020). A few studies have found that accumulated NPs could cause the structure and function of the gut microbiota community in the zebrafish to be dysregulated (Qiao et al., 2021; Xie et al., 2021); however, these studies mainly focused on cells and aquatic model organisms (Gangadoo S et al., 2020; Xie et al., 2021; Liang et al., 2021; Xu et al., 2021; Vagner et al., 2022), and studies regarding the health impacts of accumulated NPs in the intestine on gut microbiota in mammals are relatively scarce. Furthermore,

the gut microbiota has been documented to be an important biological mechanism for maintaining the homeostasis of the gut-brain axis. Therefore, once the impacts of NP exposure on the gut microbiota are confirmed in mammals, we speculated that the expose could further influence the nervous system via gut-brain axis. Moreover, microbiota-derived metabolites have been demonstrated to be among the most important biological mechanisms that regulates host metabolism, which can not only provide detailed mechanisms underlying cross-talk between the host and microbiota, but also provide novel small molecule chemicals, which may be used as preventive or treatment methods (Zheng et al., 2021; Agus et al., 2021).

Therefore, based on the above evidence, it was hypothesized that chronic low-dose NP exposure can induce nervous system injury by influencing the gut microbiota through regulating the abundance of microbiota-derived metabolites. Futhermore, the study explored whether and how microbiota-derived metabolites alleviate the adverse health impacts on the nervous system induced by NPs exposure.

METHODS AND MATERIALS

Rat and PS-NPs exposure

Sixty male Sprague Dawley rats (eight-week-old) were obtained from Vital River Lab Animal Technology Co., Ltd (China) and housed in a controlled environment room (12h:12h light/dark cycle, 40%-50% humidity, and 18-22 ℃) with water and food ad libitum. The 80 nm polystyrene nanoparticles (PS-NPs) were purchased commercially from BaseLine Chromtech Research Centre (Tianjin, China). All rats were acclimated for seven days and then continuously administered PS-NPs in drinking water at 0, 50, and 100 μg/L doses for 24 weeks. The exposure doses in our study were calculated based on the exposure dose of humans and previous studies (Xu et al., 2021; Hwang et al., 2022). Body weight and food intake were recorded twice a week. At 12 weeks and 24 week of age, the rats were arranged for behavioral tests. At 24 weeks of age, the rats were anesthetized with phenobarbital sodium and the blood, amygdala, intestinal contents, and other tissues were collected, weighed, rapidly frozen in liquid nitrogen and stored. In addition, after the rats were exposed to PS-NPs for 30 weeks, 1% dihydrochalcone (NHDC) was added to the normal diet, the rats were treated for 4 weeks, and the blood and amygdala were collected for further experiments. All animal experiments were approved by the Medical Ethics Committee of Harbin Medical University and were performed according to the Guide for Care experiment (ethics number: 2015138).

Behavioral experiments

Elevated plus-maze test

Anxiety-like behavior was determined by the elevated plus-maze test as previously described (Kraeuter AK et al., 2019). The elevated plus-maze consists of two opposite open arms and two opposite closed arms. Before the experiment, eight rats from each group were placed in an open field to acclimatize for 5 min and were then placed in the middle of the maze. The number of entries into the open and closed arms and the stay time of each arm within 5 min were recorded. The percentage of the times that rats entered the open arms and the time spent in the open arms were calculated as the main indices of the experiment.

Open field test

Anxiety-like behavior was also determined by the open field test as previously described (Kuniishi H. et al., 2019). Briefly, after acclimation for 3 h, eight rats from each group were placed in the central area of the field (100 cm×100 cm×60 cm) in sequence with their backs to the experimenter. The movement trajectory of rats in the field was recorded for 5 min. The indicators of the total distance traveled and the immobility time in the central area were calculated.

Sucrose preference test

Depression-like behavior was determined by the sucrose preference test as previously described (Iñiguez SD et al., 2014). The sucrose preference test involves an adaptation training part and a test part. In the adaptation training, eight rats from each group were placed in two bottles of 1% (W/V) sucrose solution for the first 24 h, and then one of the bottles was replaced with water for the next 24 h. During the training process, the positions were changed every 12 h. In the test part, two bottles

were weighed before consumption and after consumption for 12 h. The sucrose preference index was identified as the percentage of sucrose solution consumed versus the total amount consumed.

Shuttle box test

Cognition and memory functions were determined by the shuttle box test as previously described (Jiang et al., 2017).The shuttle box test involved a training phase and test phase. Briefly, eight rats from each group were habituated, and then subjected to 60 avoidance trials in each session per day. The rats were trained for 5 consecutive days and tested on Day 6. The conditioned light stimulus was 10 s in duration and the unconditioned stimulus was a 0.5-1.0 mA electrical shock that did not exceed 10 s. The number of conditioned responses and lack of responses were recorded.

Step-down test

Cognition and memory functions were also assessed by a step-down test as previously described (Wang et al., 2020). The step-down tests included training and passive avoidance sessions. During the training, the rats were placed in the box for 5 min, during which they could move freely. A 36 V foot shock was then administered through the bar. The stimulated rat jumped onto the platform and was immediately punished by another foot shock once it jumped down. The time it took to step down and error times were recorded.

Histomorphology assay

For histomorphology assessments, the amygdaloid nucleus and colon (six samples in each group) were dehydrated with 4% paraformaldehyde (PFA), processed

transparently with alcohol and xylene, and then dipped and embedded with paraffin. A series of sections (4 μm) were stained with HE and observed under a light microscope (Olympus, Tokyo, Japan). Histological examination was performed by blind observation to determine the number of damaged neurons under 5 view-fields with 800× microscopic magnification.

ELISAs analysis

The levels of inflammation factors (TNF-α, IL-6, IL-1β), apoptosis index (Caspase3, BAX, Bcl-2) and neurotransmitters (5-HT, DA, NE) in the serum, supernatant of the amygdaloid nucleus and colon (six samples in each group) were determined by ELISAs (Jiangsu Meimian Industrial Co., Ltd, China) according to the manufacturer's instructions, and the corresponding product numbers are listed in the Supplementary Table 1. All samples were analyzed in triplicate. The coefficients of variation within and between batches were less than 10% and 12%, respectively. The ELISAs results were examined by a microplate reader at an absorbance of 450 nm.

Proteomics analysis

Briefly, the protein was extracted from the amygdaloid nucleus (six samples from each group), and then enzymatically digested and labeled with an iTRAQ Reagent 8-plex Kit. Next, we combined all iTRAQ-labeled samples into a mixture for liquid chromatography-tandem mass spectrometry (LC-MS/MS) to separate different peptides, and a Q-Exactive mass spectrometer was used for mass spectrometry analysis and to identify the separated peptides. Differential analysis was performed using raw protein data with a false discovery rate of less than 0.05. Finally,

differential proteins were submitted to the DAVID database for enrichment analysis.

Metagenomic analysis

First, DNA was extracted from rat feces (six rats from each group), and the Nextera XT DNA Sample Prep Kit (Illumina) was used to construct the sequencing library. In addition, metagenomic sequencing was performed on the Illumina HiSeq platform and MOCAT2 V2.0 software was used for a quality control of the original sequencing data. Then, principal coordinate analysis (PCoA) analysis with Bray-Curtis PERMANOVA was used to explore the cohesion of each sample group, α-diversity was analyzed by calculating the Simpson, Chao, ACE and Shannon indices (Carter SJ et al., 2019) and the β-diversity, which is described as intersample diversity, was measured using the UniFrac distance metric (Lozupone C et al., 2005). In addition, Adonis analysis was used to show significant differences among the different groups. The functional differences were further analyzed by Kyoto Encyclopedia of Genes and Genomes (KEGG) pathway analysis and Gene Ontology (GO) function analysis.

Metabolomics analysis

Targeted metabolomics was performed to identify the different metabolites in the feces and amygdaloid nucleus (six rats in each group). Intestinal contents (500 mg) or amygdaloid nuclei (200 mg) were extracted from the rats, and an optimized technological platform for analysis was established by ULTRA-performance liquid chromatography-quadrupole time-of-flight tandem mass spectrometry (UPLC-QTOF-MS). PCA with KMO and bartlett's sphericity test was used to

demonstrate differences between control group and PS-NPs group. Then, the differential metabolites were screened by analyzing the raw data to screen the potential endogenous metabolites. All the raw data were analysesd in the Cloud Platform of BIOMARKER Techonogies Co., Ltd (Beijing, China) (http://www.biocloud.net/).

Western blot analysis and RT-PCR assay

For western blot analysis, the total proteins from the rat amygdaloid nucleus were extracted with RIPA lysis buffer (Beyotime, Shanghai) plus phenylmethanesulfonyl fluoride (Beyotime, Shanghai) and denatured by heating. The protein samples (30 μg) were loaded on a 10% SDS-PAGE gel and separated by electrophoresis. Then, the proteins were transferred to polyvinylidene fluoride membranes and blocked with 5% of skim milk. The primary antibodies, including anti-cAMP (1:800; Abcam), anti-PKA (1:800; Abcam), anti-p-CREB (1:1500; Abcam), and anti-PMCA2 (Atp2b2) (1:1000; Abcam) were incubated overnight at 4 °C. Finally, the membranes were incubated with AKP-conjugated secondary antibody (1:7500; Promega, USA) at 37 °C for 1 h. ImageJ software was used to analyze the densitometric quantification of the protein bands.

For real-time PCR, TRIzol® reagent (Solarbio, China) was used to isolate total RNA samples from the amygdaloid nucleus and synthesize cDNA with the SYBR Premix Ex Taq II Reagent Kit and gDNA Eraser according to the manufacturer's instructions (TaKaRa, Japan). Then, Power SYBR Green PCR Master Mix and 500 Real-Time PCR System of Applied Biosystems were used to evaluate the expression

of cAMP, PKA, and Atp2b2. The primer sequences were as follows: cAMP (forward: CGCTCACTGTCACTGCTATTG; reverse: CTCGGAACCTCACATACTTGG); PKA (forward: AGGTGACAGACTTCGGTTTTG; reverse: GCTTTGTTGTAGCCTTTGCTC); Atp2b2 (forward: CCAAGGTGGGGCAGAAGAT; reverse: TTGAAGGCTGTGACGAGGAC); β-actin (forward: GAGAGGGAAATCGTGCGT; reverse: GGAGGAAGAGGATGCGG).

Immunohistochemical analysis

For immunohistochemical analysis, six samples in each group were deparaffinized and hydrated with xylene and ethanol, and a 3% hydrogen peroxide solution was used for antigen repair. Goat serum was used to block the nonspecific binding sites. Then, the sections were incubated with anti-ZO-1, and anti-Claudin-1 antibodies at 4 °C overnight, and the secondary antibody was incubated for 20 min. Next, the sections were washed with PBS and observed with an optical microscope (Olympus, Tokyo, Japan). For semiquantitative counting of immunopositive cells, five fields of view were counted at 800× magnification for each sample.

Statistical analysis

Statistical data from this study are expressed as the mean±standard deviation. For the data of behavior tests, histomorphology assays, ELISAs analysis, and molecular biology experiment, the comparisons among multiple groups were performed using a one-way ANOVA test followed by Dunnett's multiple comparison test, before which the normality and homogeneity of the data were confirmed. For the multiple omics

data, the comparisons between the control group and PS-NPs group were performed using Student's t test. One-way ANOVA and student's t test were performed with R software (version 4.0.2). Two-sided P values were used in all tests and were considered statistically significant when $P<0.05$.

RESULTS

Characterization of PS-NPs and development of rats

The transmitted electron microscope image showing the PS-NPs is provided in Figure 1A. As seen in Figure 1B, according to dynamic light scattering, the water power size of PS-NPs did not change significantly, indicating that the PS-NPs were stable in the scattered water. As seen in Figure 1C, Fourier's infrared spectrum was used to identify the chemical composition. The peaks at 3362.61 cm^{-1} represented the C-H of the monosubstituted benzene component, the peak at 1636.36 cm^{-1} corresponded to the double-carbon bond, and the peak at 590.51 cm^{-1} represented the C-H. In Figure 1D, we used a Zeta Nano ZS to determine the charge of PS-NPs. The zeta potential of PS-NPs is -40.1 MV, indicating that the charge of the PS-NPs suspension liquid may not exhibit a sufficiently large charge. To achieve a stable PS-NPs suspension, sodium dodecyl sulfate (SDS) was appropriately added to expand the space block to increase the effective exclusion between the NPs.

The whole study design is presented in Figure.1E. The somatic parameter results showed that from 20 weeks of age, exposure to 50 and 100 μg/L PS-NPs significantly changed the food intake and body weight of the rats (Figure 1F, G). In addition, regardless of the dose, a non-significant impact on the organ coefficients of all tissues was observed, which were only slightly increased compared to that of the control (Figure 1H). Importantly, these results suggested that exposure to environmentally relevant concentrations of PS-NPs may have adversely affected the growth of rats.

Alteration of neurobehavior and histomorphology and biological indices of

amygdaloid nucleus

In the elevated plus-maze, open field test, and sucrose preference test, after 12 weeks of exposure, no significant differences in the various kinds of neurobehavioral indicators was observed among these groups (All $P>0.5$, Figure 2A-I). However, at the end of the exposure (24 weeks), in the PS-NPs group, the percentage of time remaining in the open arm and number of entries into the open arm decreased significantly compared with those of the control ($P<0.01$, $P<0.01$, Figure 2J, K). The total distance of movement and the sucrose preference index in the PS-NPs group were significantly lower than those in the control group ($P<0.05$, Figure 2L-N). However, in the shuttle box test and step-down test, there were no significant differences in the step latency and error frequency even after exposure for up to 24 weeks ($P>0.05$, Figure 2O, R). The HE staining results showed pyknosis and hyperchromatism of neurons were observed in the amygdala of PS-NPs-exposed rats, whereas the amygdala neurons in the control group showed normal morphology (Figure 2S). In addition, in the PS-NPs group, the expression of genes related to neuroinflammation and apoptosis in the amygdaloid nucleus and serum changed significantly compared to control group (Figure 2T, U). Combined, these results demonstrated that PS-NPs exposure could stimulate neuroinflammation and apoptosis and then induce the impairment of amygdaloid nucleus structure and anxiety-related behavior.

Cross-analysis of intestinal flora analysis and targeted metabolomics in feces

The HE staining results for the colon showed that the intestinal fluff was sparse,

shorter, and even disappeared and inflammatory cell infiltration, capillary proliferation could be also observed in the PS-NPs group (Figure 3A). The morphologic changes were assessed and graded on a scale of 0-5 using the intestinal injury score (Chiu CJ et al., 1970; Ji J. et al., 2018; Yang J., et al., 2021; Petrat F., et al., 2010). And the intestinal injury score was significantly higher than that in the control group (Figure 3D). In addition, the expression of colorectal tight junction proteins and serum lipopolysaccharide (LPS) was measured, and it was found that ZO-1 and claudin-1 levels were significantly reduced (Figure 3B, C), while serum LPS was markedly increased after long-term PS-NPs exposure (Figure 3E), which indicated that the intestinal barrier function was impaired. Previous studies have demonstrated that gut microbiota plays an important role in brain processes, forming the basis of the gut-brain axis (Morais et al., 2021; Quigley, 2017). Therefore, we performed the intestinal microbiome analysis following exposure to PS-NPs. PCoA results showed that PS-NPs exposure could significantly disrupt the balance of the intestinal microbiome (Figure 3F). The ACE index (P=0.00044) and Chao1 index (P=0.0046) were significantly increased, indicating that the richness of the intestinal microbiota increased (Figure 3G), in addition to the rarefaction curves (Supplementary Figure 2), whereas the Shannon index (P=0.066) and Simpson index (P=0.0099) were decreased indicating that the overall community diversity decreased (Figure 3G). And Figures 3I and J showed the change in microbial composition at the phylum level and genus level. Moreover, LEfSe analysis showed that all 101 changed genera could be identified as biomarkers to distinguish the PS-NPs and control groups

(Figure 3H). Specifically, the relative abundances of *Bacteroides* (6.08-fold), *Paraprevotella* (4.91-fold), *Mucispirillum* (34.07-fold), and *Helicobacter* (2.45-fold) were significantly increased, while *Oscillibacter* (0.30-fold) and *Ruminococcus* (0.10-fold) were markedly decreased (Figure 3M). The heatmap analysis of the correlation coefficient showed that *Firmicutes (Acetatifactor, Ruminococcus, Oscillibacter), Bacteroidetes (Bacteroides, Paraprevotella)* and *Proteobacteria (Azospirillum, Helicobacteraceae)* were highly positively or negatively correlated with each other (Figure 3L).

In addition, the UPLC/Q-TOF MS/MS platform was also used to identify the different metabolites in feces. The PCA results indicated that the PS-NPs group and control group exhibited significant differences (Figure 4A). A total of 122 changed metabolites were finally identified in the feces (Figure 4B) and the metabolites of the top 10 of the fold-change are presented in Figure 4D. The differential metabolites were enriched in the metabolic pathways of valine, leucine, and isoleucine degradation, tryptophan metabolism, central carbon metabolism in cancer, phenylalanine, tyrosine, and tryptophan biosynthesis (Figure 4E). Compared to that of control, N-acetylserotonin, dimethylglycine, 3-phenylpyruvic-Acid, beta-Alanine, 4-aminobutyric-acid, N-acetyl-L-tyrosine, and dihydrocaffeic-acid were significantly decreased, and deoxycorticosterone, 3-N-methyl-L-histidine, glycocholic-acid, and stearoyl-carnitine were significantly increased in the feces of the PS-NPs group (Figure 4C). To explore the intrinsic interaction between metabolites and intestinal microbiota, the associations between altered metabolites (top 30) in the feces and

different intestinal microbiota (top 30) were further investigated (Figure 4F). The correlation analysis results showed that these changed metabolites in the feces were highly associated with changes in the *Proteobacteria, Firmicutes, and Bacteroidetes*. All the metabolic and microbial variables were clustered into different modules using weighted gene coexpression network analysis (Figure 4G). The correlation between selected modules was performed using the Pearson method (Figure 4H), and the importance score of each module is shown in Figure 4I. The correlations of the important metabolome and microbiome modules and their affiliations are presented in the mulberry plot (Figure 4J). The associations between intestinal flora and metabolites are shown in Supplementary Figure1. Significant relationships between *Bacteroides, Oscillibacter* and the metabolite N-acetyl-L-tyrosine (R=-0.62, *P*=0.030; R=0.67, *P*=0.017), 4-aminobutyric-acid (R=-0.61, *P*=0.030; R=0.78, *P*=0.003), corticosterone (R=0.58, *P*=0.049; R=-0.53, *P*=0.075), deoxycorticosterone (R=0.59, *P*=0.045; R=-0.63, *P*=0.028), N-acetylserotonin (R=-0.59, *P*=0.042; R=0.78, *P*=0.003) could be observed. And importantly, dihydrocaffeic-acid, which exhibited the maximum fold-change, was significantly associated with all these intestinal flora (*Bacteroides* (R=-0.86, $P=3.6\times10^{-4}$), *Paraprevotella* (R=-0.78, *P*=0.003), *Mucispirillum* (R=-0.58, *P*=0.046), *Helicobacter* (R=-0.59, *P*=0.044), *Oscillibacter* (R=0.87, $P=2\times10^{-4}$), and *Ruminococcus* (R=0.71, *P*=0.01)) (Supplementary Figure 1).

Cross-analysis of targeted metabolomics in the amygdaloid nucleus and feces

To elucidate the underlying mechanism of the gut-brain axis, the targeted metabolomics analysis was also performed in the amygdaloid nucleus, as well as the

cross-analysis with the metabolomics of feces. In the metabolomics analysis for the amygdaloid nucleus, partial least squares discriminant analysis (PLS-DA) score plots showed a noteworthy difference in the metabolic profiles of the amygdaloid nucleus between the control and PS-NPs groups in both positive and negative ion modes (Figure 5A). The heatmap figure shows the perspective of the top 20 different metabolites (Figure 5B). The differential metabolites were enriched in the nervous system and neurodegenerative diseases (Figure 5C) and multiple neurotransmitter-related pathways, including the sphingolipid signaling pathway, sphingolipid metabolism, and ATP-binding cassette transporters (Figure 5D). The associations between the differential amygdaloid nucleus metabolites and different abundances of intestinal flora (Figure 5E) and differential metabolites of feces (Figure 5H) are shown. N-phenylacetylaspartic acid and N-stearoylsphingosine were significantly associated with *Bacteroides* (R=0.69, *P*=0.012; R=0.62, *P*=0.031), *Oscillibacter* (R=-0.83, $P=8.2\times10^{-4}$; R=0.78, *P*=0.003), *Ruminococcus* (R=-0.75, *P*=0.005; R=0.39, *P*=0.22), *Paraprevotella* (R=0.58, *P*=0.047; R=-0.65, *P*=0.023), *Helicobacter* (R=0.69, *P*=0.014; R=-0.44, *P*=0.15), N-Acetyl-L-Tyrosine (R=-0.54, *P*=0.067; R=0.79, *P*=0.002), Stearoyl-carnitine (R=0.64, *P*=0.026; R=-0.62, *P*=0.031), 4-Aminobutyric-Acid (R=-0.74, *P*=0.006; R=0.63, *P*=0.027), N-Acetylserotonin (R=-0.32, *P*=0.31; R=-0.61, *P*=0.037) (Figure 5F, I). The dihydrocaffeic-acid was significantly associated with N-Phenylacetylaspartic acid (R=-0.83, $P=8.3\times10^{-4}$), N-Phenylacetylphenylalanine (R=0.71, *P*=0.009), N-Stearoylsphingosine (R=0.72, *P*=0.008), Deoxycholic acid (R=0.57, *P*=0.05), 4-Hydroxydiphenylamine (R=-0.69,

P=0.013) (Figure 5I). And the heatnetwork and sankey plot showed the correlations between individual omics and phenotypes (Figure 5G, J), which illustrated that there were significant positive or negative correlations among the gut microbiota, fecal metabolites, amygdala metabolites, inflammatory responses, and apoptotic processes. Network analysis showed that dihydrocaffeic acid was located at the center of the network (Figure 5K).

Dihydrocaffeic acid alleviated PS-NPs-induced neuroinflammation and apoptosis

As NHDC could be degraded into dihydrocaffeic acid by intestinal microbiota after oral consumption, so we reversed the adverse effects of the PS-NPs rat model with NHDC. ELISAs results in the serum and amygdala showed that after treatment for one month, inflammatory factors (TNF-α, IL-1β, IL-6), apoptosis indices (BAX, Bcl-2, caspase3), and neurotransmitters (5-HT, DA, NE) were significantly improved (Figure 6A, B). To elucidate the underlying mechanism, proteomics was performed in the amygdaloid nucleus. The results showed that 46 differentially expressed proteins (11 down-regulated and 35 up-regulated) were identified in the PS-NPs+NHDC group compared to the PS-NPs group (Figure 6C). GO analysis results indicated that differentially expressed proteins were enriched in cranial nerve structural organization, inflammation response (leukocyte cell-cell adhesion, leukocyte aggregation, astrocyte development), and ion transport (regulation of metal ion transport, potassium ion transport, response to zinc ion) (Figure 6D). KEGG pathway analysis showed that differentially expressed proteins were mainly enriched in mineral absorption and multiple signaling pathways (cGMP-PKG signaling pathway, calcium signaling

pathway, cAMP signaling pathway, and IL-17 signaling pathway) (Figure 6E). Enrichment plots obtained by Gene Set Enrichment Analysis (GSEA) showed that the majority of the synapse and synapse part-associated genes were upregulated in the PS-NPs+NHDC group compared to the PS-NPs group (Figure 6F). Network analysis showed that Atp2b2 was identified as the hub gene, as Atp2b2 exhibited the greatest number of gene-gene connections (Figure 6G). Atp2b2 plays an essential role in maintaining calcium homeostasis in neurons and accumulative evidence has suggested that downregulation of Atp2b2 is an important and specific contributor to the impairment of neuronal vulnerability (Martín-de-Saavedra et al., 2022; Brendel et al., 2014; Mirabelli et al., 2019). The reduced PKA dependent on cAMP may be a possible molecular link between p-CREB level and Atp2b2 expressions (Baggaley et al., 2007; Ramos-Alvarez et al., 2019). Our results also demonstrated that the gene levels and protein expressions levels of the cAMP/PKA/p-CREB/Atp2b2 signaling pathway were significantly increased after treatment with dihydrocaffeic acid (Figure 6H-J).

DISCUSSION

Based on multi-omics analyses that combined a series of in vivo and in vitro experiments, this study found that long-term exposure to low-dose PS-NPs could induce an impairment in the amygdaloid nucleus and anxiety-like behaviors in rats by influencing the structure of the gut microbiota including the upregulation of the abundance of *Bacteroidetes, Proteobacteria* and *Defferibacteres,* and downregulation of *the* abundance of *Firmicutes*. Furthermore, the aberrant gut microbiome resulted in a decrease in dihydrocaffeic acid, and an increase in stearoylcarnitine, which mediated the deleterious effects of PS-NPs exposure through the microbiota-brain axis. This study also found that dihydrocaffeic-acid exposure could alleviate the apoptosis and neuroinflammation by downregulating the cAMP/PKA/p-CREB/Atp2b2 signaling pathway.

To the best of our knowledge, this study is the first to examine the health impacts of long-term and low-dose exposure of PS-NPs in mammals. Because previous studies have documented that PS-NPs derived from food container are frequently detected (Lambert and Wagner, 2016; Jiang et al., 2020; Kumar R et al., 2022), this study selected the drinking water as the exposure pathway. During the experiments, we observed that the rats in the PS-NPs group showed significant symptoms of anhedonia and a significant reduction in exploratory behavior, but their learning and memory abilities were not significantly affected, although there was a decreasing trend. The amygdaloid is responsible for the important emotional response and hippocampal damage could be reflected by the spatial memory and cognitive function

(Šimić et al., 2021; Chauhan et al., 2021). Furthermore, the neuroethology and histomorphology results also showed that the deleterious effects of PS-NPs exposure were more serious in the amygdaloid nucleus than in the hippocampus. These results suggested that PS-NPs exposure may be more accessible to damage to the amygdaloid nucleus, not the hippocampus.

These above observations led us to explore how PS-NPs exposure induced these deleterious health impacts. In our study, the intervention method for PS-NPs was gastric intervention, and previous studies have documented that most ingested PS-NPs cannot be digested (Brandts et al., 2022; Meng et al., 2022), which may be more available for gut microbiota. Furthermore, there is growing evidence for the impact of gut microbiota on neuropsychiatric disorders, such as depression and anxiety (Bear et al., 2020; Fond et al., 2020). Based on these previous studies, we therefore performed the metagenomics analysis to directly assess whether an abnormal gut microbiome played a crucial role in the adverse effects of long-term PS-NPs exposure. We observed four altered phyla (*Bacteroidetes*, *Proteobacteria*, *Firmicutes*, and *Defferibacteres*) and 101 changed genera in the rats after long-term PS-NPs exposure. These findings were consistent with the previous study conducted in zebrafish (Yu et al., 2022), which also found that PS-NPs exposure could reduce the relative abundance of *Firmicutes* and increase the relative abundance of *Proteobacteria* in zebrafish. Both *Proteobacteria* and *Firmicutes* have been found to induce the dysfunction of immune homeostasis, causing the brain−intestine−microbiota axis to be disrupted (Teng et al., 2022). In contrast to the study using an aquatic model, we

also specifically identified *Defferibacteres* at the phylum level and its subgenus, *Mucispirillum* in the mammal models. A few studies have shown that *Mucispirillum* could induce the progressive apoptosis of neurons such as dopamine, promote the release of inflammatory substances and affect the progression of the nervous system (Sticlaru et al., 2019; Rincel et al., 2019), further supporting our findings.

Because accumulating studies have demonstrated that the metabolites produced by the gut microbiota play central roles in the cross-talk between the microbiota and host brain (Janik et al., 2016; Chudzik et al., 2021), we further examined the profiles of metabolites in feces, and we found that long-term PS-NPs exposure could result in significant changes in microbial amino acid, lipid metabolism and neurotransmitter-related pathways in feces. Among the different metabolites in the feces, dihydrocaffeic acid and stearoylcarnitine with the biggest fold-change were strongly associated with hub intestinal microbiota. Previous studies demonstrated that dihydrocaffeic acid is a strong antioxidant in vivo by decreasing intracellular reactive oxygen species and extracellular H_2O_2 production, enhancing the activities of catalase and superoxide dismutase (Gutierrez-Zetina et al., 2021; Oliveira et al., 2019; Martini et al., 2019). An increased concentration of stearoylcarnitine could induce caspase activity indirectly, and cause mitochondrial neurodegeneration (Li et al., 2013), which supported the deleterious effects of PS-NPs exposure on amygdaloid nucleus.

Furthermore, to provide more comprehensive evidence regarding the impacts of PS-NPs exposure on amygdaloid nucleus impairments through the microbiota-brain axis, we also examined the metabolites in the amygdaloid nucleus. We found that

among the metabolites in feces, the association between dihydrocaffeic acid and crucial metabolites in the amygdaloid nucleus, including deoxycholic acid, 4-hydroxydipheny, and N-phenylacetylaspartoc acid, was the strongest. Moreover, the results of multiomics analysis also showed that dihydrocaffeic-acid played a central role, which could be linked to both gut bacteria and amygdala metabolites. Taken together, the above results collectively showed that long-term exposure to low-dose PS-NPs could influence the structure of the gut microbiota, decreasing the abundance of dihydrocaffeic-acid, and influencing the profiles of metabolites in amygdaloid nucleus; as a result, the amygdaloid nucleus is impaired through the induction of neuroinflammation and apoptosis.

Because the decreased abundance of dihydrocaffeic-acid plays a central role in regulating the deleterious effects of PS-NPs through gut microbiota, we were also interested in examining whether the dihydrocaffeic-acid levels could be rescued as an intervention method for treating PS-NPs exposure. Previous studies have reported that dihydrocaffeic acid can be derived by NHDC through intestinal microbiota after oral consumption, which is a metabolite in polyphenol foods, beverages, and medicinal plants (such as chocolate, coffee, and wine extracts). After supplementation with NHDC and PS-NPs exposure, we observed that neuroinflammation and apoptosis in the amygdaloid nucleus were significantly alleviated. To elucidate the potential mechanism, we performed proteomics, and identified the Atp2b2 gene as the central gene that was enhanced by dihydrocaffeic-acid.

This study provided evidence for the health outcomes, prevention methods and

treatment strategies regarding long-term exposure to PS-NPs, and the importance of environmental management and food safety were emphasized. Macromolecular plastics can breakdown into microplastics and nanoplastics through mechanical wear, ultraviolet radiation, and biodegradation. Studies have found that microplastics and nanoplastics are abundant in the atmosphere, water and soil and other natural environments, which are accessible to animals or humans through food, drinking water, etc., posing a potential threat to health. Therefore, our findings are important for environmentalists, nutritionists, policy-makers and public health endeavors, such as developing an accurate database to disclose the content of PS-NPs in specific food ingredient lists or recommending some foods rich in dihydrocaffeic acid.

In conclusion, our findings suggested that PS-NPs exposure could induce the dysfunction of neurobehaviors as well as change the composition and function of the microbiome in rats. The underlying mechanism of this toxicity involves disruption of the metabolite-mediated gut-brain axis. More importantly, dihydrocaffeic acid could alleviate these adverse effects by ameliorating neuroinflammation and apoptosis. Our results showed how PS-NPs exposure could disturb the regulation of the intestinal-microbiota-brain pathway which should be considered when evaluating the environmental health risks of PS-NPs to mammals or humans.

.

AUTHOR INFORMATION

Wenbo Jiang−Department of Nutrition and Food Hygiene, the National Key Discipline, School of Public Health, Harbin Medical University, Harbin, P. R. China.

Cong Hu − Department of Nutrition and Food Hygiene, the National Key Discipline, School of Public Health, Harbin Medical University, Harbin, P. R. China.

Yunyan Chen−Department of Nutrition and Food Hygiene, the National Key Discipline, School of Public Health, Harbin Medical University, Harbin, P. R. China.

Xinyi Sun−Department of Nutrition and Food Hygiene, the National Key Discipline, School of Public Health, Harbin Medical University, Harbin, P. R. China.

Huanyu Wu−Department of Nutrition and Food Hygiene, the National Key Discipline, School of Public Health, Harbin Medical University, Harbin, P. R. China.

Ruiming Yang−Department of Nutrition and Food Hygiene, the National Key Discipline, School of Public Health, Harbin Medical University, Harbin, P. R. China.

Fengru Niu−Department of Nutrition and Food Hygiene, the National Key Discipline, School of Public Health, Harbin Medical University, Harbin, P. R. China.

Yiwei Tang−Department of Nutrition and Food Hygiene, the National Key Discipline, School of Public Health, Harbin Medical University, Harbin, P. R. China.

Author Contributions

Wei Wei, Cong Hu, Yue Li, Tianshu Han, Changhao Sun and Wenbo Jiang contributed to the literature search. Wei Wei, Tianshu Han, and Wenbo Jiang designed the study. Yunyan Chen, Xinyi Sun, Huanyu Wu, and Ruiming Yang performed the experiments.

Huanyu Wu, Fengru Niu, and Yiwei Tang analyzed the data. Wei Wei, Cong Hu, and Wenbo Jiang wrote and corrected the manuscript. All authors reviewed and approved the final manuscript.

Competing interest

The authors declare no competing financial interest.

ACKNOWLEDGMENTS

This research was supported by funds from HMU Marshal Initiative Funding (HMUMIF-21010 to Wenbo Jiang), China Postdoctoral Science Foundation Funded Project (2021M701021 to Wenbo Jiang), and Heilongjiang Province Postdoctoral Science Foundation Funded Project (LBH-Z21073 to Wei Wei).

REFERENCES

Agus A, Clément K, Sokol H. Gut microbiota-derived metabolites as central regulators in metabolic disorders. Gut 2021; 70: 1174-1182. https://doi.org/10.1136/gutjnl-2020-323071.

Baggaley E, McLarnon S, Demeter I, Varga G, Bruce JI. Differential regulation of the apical plasma membrane Ca(2+) -ATPase by protein kinase A in parotid acinar cells. J Biol Chem 2007; 282: 37678-93. https://doi.org/10.1074/jbc.M703416200.

Banerjee A, Shelver WL. Micro- and nanoplastic induced cellular toxicity in mammals: A review. Sci Total Environ 2021;755(Pt 2):142518. https://doi:10.1016/j.scitotenv.2020.142518.

Bear TLK, Dalziel JE, Coad J, Roy NC, Butts CA, Gopal PK. The Role of the Gut Microbiota in Dietary Interventions for Depression and Anxiety. Adv Nutr 2020; 11: 890-907. https://doi.org/10.1093/advances/nmaa016.

Brandts I, Cánovas M, Tvarijonaviciute A, Llorca M, Vega A, Farré M, et al. Nanoplastics are bioaccumulated in fish liver and muscle and cause DNA damage after a chronic exposure. Environ Res 2022; 212: 113433. https://doi.org/10.1016/j.envres.2022.113433.

Brendel A, Renziehausen J, Behl C, Hajieva P. Downregulation of PMCA2 increases the vulnerability of midbrain neurons to mitochondrial complex I inhibition. Neurotoxicology 2014; 40: 43-51. https://doi.org/10.1016/j.neuro.2013.11.003.

Carter SJ, Hunter GR, Blackston JW, Liu N, Lefkowitz EJ, Van Der Pol WJ, et al. Gut microbiota diversity is associated with cardiorespiratory fitness in post-primary

treatment breast cancer survivors. Exp Physiol 2019; 104: 529-539. https://doi.org/10.1113/ep087404.

Chauhan NR, Kumar R, Gupta A, Meena RC, Nanda S, Mishra KP, et al. Heat stress induced oxidative damage and perturbation in BDNF/ERK1/2/CREB axis in hippocampus impairs spatial memory. Behav Brain Res 2021; 396: 112895. https://doi.org/10.1016/j.bbr.2020.112895.

Chiu CJ, McArdle AH, Brown R, Scott HJ and Gurd FN. (1970). Intestinal mucosal lesion in low-flow states. I. A morphological, hemo -dynamic, and metabolic reappraisal. Arch Surg 101 478-483. https://doi: 10.1001/archsurg.1970.01340280030009.

Chudzik A, Orzyłowska A, Rola R, Stanisz GJ. Probiotics, Prebiotics and Postbiotics on Mitigation of Depression Symptoms: Modulation of the Brain-Gut-Microbiome Axis. Biomolecules 2021; 11. https://doi.org/10.3390/biom11071000.

Fond GB, Lagier JC, Honore S, Lancon C, Korchia T, Sunhary De Verville PL, et al. Microbiota-Orientated Treatments for Major Depression and Schizophrenia. Nutrients 2020; 12. https://doi.org/10.3390/nu12041024.

Gangadoo S, Owen S, Rajapaksha P, et al. Nano-plastics and their analytical characterisation and fate in the marine environment: From source to sea. Sci Total Environ. 2020;732:138792. https://doi:10.1016/j.scitotenv.2020.138792.

Gutierrez-Zetina SM, González-Manzano S, Ayuda-Durán B, Santos-Buelga C, González-Paramás AM. Caffeic and Dihydrocaffeic Acids Promote Longevity and Increase Stress Resistance in Caenorhabditis elegans by Modulating Expression of

Stress-Related Genes. Molecules 2021; 26. https://doi.org/10.3390/molecules26061517.

Hernandez L, Xu E, Larsson H, Tahara R, Maisuria V, Tufenkji N. Plastic Teabags Release Billions of Microparticles and Nanoparticles into Tea. Environmental science & technology 2019; 53: 12300-12310. https://doi.org/10.1021/acs.est.9b02540.

Hirt N, Body-Malapel M. Immunotoxicity and intestinal effects of nano- and microplastics: a review of the literature. Particle and fibre toxicology 2020; 17: 57. https://doi.org/10.1186/s12989-020-00387-7.

Hwang KS, Son Y, Kim SS, Shin DS, Lim SH, Yang JY, et al. Size-Dependent Effects of Polystyrene Nanoparticles (PS-NPs) on Behaviors and Endogenous Neurochemicals in Zebrafish Larvae. Int J Mol Sci 2022; 23. https://doi.org/10.3390/ijms231810682.

Iñiguez SD, Riggs LM, Nieto SJ, Dayrit G, Zamora NN, Shawhan KL, et al. Social defeat stress induces a depression-like phenotype in adolescent male c57BL/6 mice. Stress 2014; 17: 247-55. https://doi.org/10.3109/10253890.2014.910650.

Janik R, Thomason LAM, Stanisz AM, Forsythe P, Bienenstock J, Stanisz GJ. Magnetic resonance spectroscopy reveals oral Lactobacillus promotion of increases in brain GABA, N-acetyl aspartate and glutamate. Neuroimage 2016; 125: 988-995. https://doi.org/10.1016/j.neuroimage.2015.11.018.

Ji, J., Gu, Z., Li, H., Su, L., & Liu, Z. (2018). Cryptdin-2 predicts intestinal injury during heatstroke in mice. International journal of molecular medicine, 41(1), 137–146. https://doi: 10.3892/ijmm.2017.3229.

Jiang B, Kauffman AE, Li L, McFee W, Cai B, Weinstein J, et al. Health impacts of environmental contamination of micro- and nanoplastics: a review. Environ Health Prev Med 2020; 25: 29. https://doi.org/10.1186/s12199-020-00870-9.

Jiang W, Chen Y, Li B, Gao S. DBA-induced caspase-3-dependent apoptosis occurs through mitochondrial translocation of cyt-c in the rat hippocampus. Mol Biosyst 2017; 13: 1863-1873. https://doi.org/10.1039/c7mb00246g.

Kraeuter AK, Guest PC, Sarnyai Z. The Elevated Plus Maze Test for Measuring Anxiety-Like Behavior in Rodents. Methods Mol Biol 2019; 1916: 69-74. https://doi.org/10.1007/978-1-4939-8994-2_4.

Kumar R, Manna C, Padha S, et al. Micro(nano)plastics pollution and human health: How plastics can induce carcinogenesis to humans?. Chemosphere. 2022;298:134267. https://doi:10.1016/j.chemosphere.2022.134267

Kuniishi H, Ichisaka S, Yamamoto M, Ikubo N, Matsuda S, Futora E, et al. Early deprivation increases high-learning behavior, a novel anxiety-like behavior, in the open field test in rats. Neurosci Res 2017; 123: 27-35. https://doi.org/10.1016/j.neures.2017.04.012.

Lambert S, Wagner M. Characterisation of nanoplastics during the degradation of polystyrene. Chemosphere 2016; 145: 265-8. https://doi.org/10.1016/j.chemosphere.2015.11.078.

Li XZ, Zhang SN, Lu F, Liu CF, Wang Y, Bai Y, et al. Cerebral metabonomics study on Parkinson's disease mice treated with extract of Acanthopanax senticosus harms. Phytomedicine 2013; 20: 1219-29. https://doi.org/10.1016/j.phymed.2013.06.002.

Liang B, Zhong Y, Huang Y, Lin X, Liu J, Lin L, et al. Underestimated health risks: polystyrene micro- and nanoplastics jointly induce intestinal barrier dysfunction by ROS-mediated epithelial cell apoptosis. Part Fibre Toxicol 2021; 18: 20. https://doi.org/10.1186/s12989-021-00414-1.

Liu S, Yan L, Zhang Y, Junaid M, Wang J. Polystyrene nanoplastics exacerbated the ecotoxicological and potential carcinogenic effects of tetracycline in juvenile grass carp (Ctenopharyngodon idella). The Science of the total environment 2022; 803: 150027. https://doi.org/10.1016/j.scitotenv.2021.150027.

Lozupone C, Knight R. UniFrac: a new phylogenetic method for comparing microbial communities. Appl Environ Microbiol 2005; 71: 8228-35. https://doi.org/10.1128/aem.71.12.8228-8235.2005.

Martín-de-Saavedra MD, Dos Santos M, Culotta L, Varea O, Spielman BP, Parnell E, et al. Shed CNTNAP2 ectodomain is detectable in CSF and regulates Ca(2+) homeostasis and network synchrony via PMCA2/ATP2B2. Neuron 2022; 110: 627-643.e9. https://doi.org/10.1016/j.neuron.2021.11.025.

Martini S, Conte A, Tagliazucchi D. Antiproliferative Activity and Cell Metabolism of Hydroxycinnamic Acids in Human Colon Adenocarcinoma Cell Lines. J Agric Food Chem 2019; 67: 3919-3931. https://doi.org/10.1021/acs.jafc.9b00522.

Meng X, Zhang J, Wang W, Gonzalez-Gil G, Vrouwenvelder J, Li Z. Effects of nano- and microplastics on kidney: Physicochemical properties, bioaccumulation, oxidative stress and immunoreaction. Chemosphere 2022; 288: 132631. https://doi.org/10.1016/j.chemosphere.2021.132631.

Mirabelli E, Ni L, Li L, Acioglu C, Heary RF, Elkabes S. Pathological pain processing in mouse models of multiple sclerosis and spinal cord injury: contribution of plasma membrane calcium ATPase 2 (PMCA2). J Neuroinflammation 2019; 16: 207. https://doi.org/10.1186/s12974-019-1585-2.

Morais LH, Schreiber HLt, Mazmanian SK. The gut microbiota-brain axis in behaviour and brain disorders. Nat Rev Microbiol 2021; 19: 241-255. https://doi.org/10.1038/s41579-020-00460-0.

Oliveira MM, Ratti BA, Daré RG, Silva SO, Truit M, Ueda-Nakamura T, et al. Dihydrocaffeic Acid Prevents UVB-Induced Oxidative Stress Leading to the Inhibition of Apoptosis and MMP-1 Expression via p38 Signaling Pathway. Oxid Med Cell Longev 2019; 2019: 2419096. https://doi.org/10.1155/2019/2419096.

Petrat, F., Swoboda, S., de Groot, H., & Schmitz, K. J. (2010). Quantification of ischemia-reperfusion injury to the small intestine using a macroscopic score. Journal of investigative surgery : the official journal of the Academy of Surgical Research, 23(4), 208-217. https://doi: 10.3109/08941931003623622.

Qiao J, Chen R, Wang M, Bai R, Cui X, Liu Y, et al. Perturbation of gut microbiota plays an important role in micro/nanoplastics-induced gut barrier dysfunction. Nanoscale 2021; 13: 8806-8816. https://doi.org/10.1039/d1nr00038a.

Quigley EMM. Microbiota-Brain-Gut Axis and Neurodegenerative Diseases. Curr Neurol Neurosci Rep 2017; 17: 94. https://doi.org/10.1007/s11910-017-0802-6.

Ramos-Alvarez I, Lee L, Jensen RT. Cyclic AMP-dependent protein kinase A and EPAC mediate VIP and secretin stimulation of PAK4 and activation of

Na(+),K(+)-ATPase in pancreatic acinar cells. Am J Physiol Gastrointest Liver Physiol 2019; 316: G263-g277. https://doi.org/10.1152/ajpgi.00275.2018.

Rincel M, Aubert P, Chevalier J, Grohard PA, Basso L, Monchaux de Oliveira C, et al. Multi-hit early life adversity affects gut microbiota, brain and behavior in a sex-dependent manner. Brain Behav Immun 2019; 80: 179-192. https://doi.org/10.1016/j.bbi.2019.03.006.

Rodrigues A, de Jesus G, Waked D, Gomes G, Silva T, Yamawake V, et al. Scientific Evidence about the Risks of Micro and Nanoplastics (MNPLs) to Human Health and Their Exposure Routes through the Environment. Toxics 2022; 10. https://doi.org/10.3390/toxics10060308.

Šimić G, Tkalčić M, Vukić V, Mulc D, Španić E, Šagud M, et al. Understanding Emotions: Origins and Roles of the Amygdala. Biomolecules 2021; 11. https://doi.org/10.3390/biom11060823.

Sticlaru L, Stăniceanu F, Cioplea M, Nichita L, Bastian A, Micu G, et al. Dangerous Liaison: Helicobacter pylori, Ganglionitis, and Myenteric Gastric Neurons: A Histopathological Study. Anal Cell Pathol (Amst) 2019; 2019: 3085181. https://doi.org/10.1155/2019/3085181.

Stock V, Laurisch C, Franke J, Dönmez MH, Voss L, Böhmert L, et al. Uptake and cellular effects of PE, PP, PET and PVC microplastic particles. Toxicol In Vitro 2021; 70: 105021. https://doi.org/10.1016/j.tiv.2020.105021.

Teng M, Zhao X, Wang C, Wang C, White JC, Zhao W, et al. Polystyrene Nanoplastics Toxicity to Zebrafish: Dysregulation of the Brain-Intestine-Microbiota

Axis. ACS Nano 2022. https://doi.org/10.1021/acsnano.2c01872.

Vagner M, Boudry G, Courcot L, Vincent D, Dehaut A, Duflos G, et al. Experimental evidence that polystyrene nanoplastics cross the intestinal barrier of European seabass. Environ Int 2022; 166: 107340. https://doi.org/10.1016/j.envint.2022.107340.

Wang Y, Jiang W, Dong Q, Zhao Y, Chen Y, Sun C, et al. Fetal exposure to dichloroacetic acid and impaired cognitive function in the adulthood. Brain Behav 2020; 10: e01801. https://doi.org/10.1002/brb3.1801.

Xie S, Zhou A, Wei T, Li S, Yang B, Xu G, et al. Nanoplastics Induce More Serious Microbiota Dysbiosis and Inflammation in the Gut of Adult Zebrafish than Microplastics. Bull Environ Contam Toxicol 2021; 107: 640-650. https://doi.org/10.1007/s00128-021-03343-8.

Xu D, Ma Y, Han X, Chen Y. Systematic toxicity evaluation of polystyrene nanoplastics on mice and molecular mechanism investigation about their internalization into Caco-2 cells. J Hazard Mater 2021; 417: 126092. https://doi.org/10.1016/j.jhazmat.2021.126092.

Yang, J., Wu, Y., Xu, Y., Jia, J., Xi, W., Deng, H., & Tu, W. (2021). Dexmedetomidine Resists Intestinal Ischemia-Reperfusion Injury by Inhibiting TLR4/MyD88/NF-κB Signaling. The Journal of surgical research, 260, 350–358. https://doi: 10.1016/j.jss.2020.11.041.

Yu Z, Zhang L, Huang Q, Dong S, Wang X, Yan C. Combined effects of micro-/nano-plastics and oxytetracycline on the intestinal histopathology and microbiome in zebrafish (Danio rerio). Sci Total Environ 2022; 843: 156917.

https://doi.org/10.1016/j.scitotenv.2022.156917.

Zheng X, Chen T, Jiang R, Zhao A, Wu Q, Kuang J, et al. Hyocholic acid species improve glucose homeostasis through a distinct TGR5 and FXR signaling mechanism. Cell Metab 2021; 33: 791-803.e7. https://doi.org/10.1016/j.cmet.2020.11.017.

Figure Legend

Figure 1. Characteristics of PS-NPs. (A) The representative image from transmission electron microscopy. (B) Particle size distribution in deionized water. (C) Zeta Potential Distribution of PS-NPs. (D) Fourier-transform infrared spectroscopy of PS-NPs. (E) The overall design of the study. (F) The effect of PS-NPs on the body weight. (G) The effect of PS-NPs on the absolute food intake. (H) The effect of PS-NPs on the organ coefficient. Data were presented as mean±SD(n=6).

Figure 2. Behavioral tests in rats between the control group and PS-NPs group. The percentage of stay time in the open arm (A,J) and number of entries into the open arm (B,K) in the elevated plus-maze test. The total distance traveled (C,L) and the immobility time in the central area (D,M) in the open field test. The sucrose preference index in the sucrose preference test (E,N). The number of conditioned responses (F,O) and lack of responses (G,P) in the shuttle box test. Step down latency(H,Q) and error times(I,R) in the step down test after 12 weeks and 24 weeks exposure. Data were presented as mean±SD (n=8). The effect of PS-NPs on histomorphology of amygdala (S). The effect of PS-NPs on the inflammation factors (TNF-α, IL-6, IL-1β), apoptosis index (Caspase3, BAX, Bcl-2) and neurotransmitters (5-HT, DA, NE) in the serum and amygdaloid nucleus(T, U). ELISAs data were presented as mean±SD (n=6).

Figure 3. The effect of PS-NPs on the histomorphology of colon (A) and the intestinal injury score (D). The effect of PS-NPs on the ZO-1 (B) and Claudin-1 (C) protein expression by immunohistochemical analysis. The effect of PS-NPs on the

serum LPS (E). Two-dimensional principal coordinate analysis plots of intestinal microbial data (F). Alpha diversity of intestine microbiota, including ACE, Chao1, Shannon, and Simpson(G). Visualization of phylum(I) and genus(J) composition distribution in the intestine microbiota. LefSe analysis between control and PS-NPs group (H,K). The heatmap of the correlation coefficient among the alter genera (L). Abundance of *Bacteroides, Helicobacter, Oscillibacter, Ruminococcus, Mucispirillum, Paraprevotella* in control and PS-NPs group (M). Data were presented as mean±SD (n=6).

Figure 4. The different metabolites between PS-NPs group and control group using PCA analysis (A). The volcano plot (B) and heatmap (C) of differential metabolites in the feces. The top 20 differential metabolites (D). GO analysis (E). Heatmap of the relationship between the intestine microbiota and metabolites (F). Importance scores of the first module in metabolome and microbiome data (G). Heatmap (H) and chord plot (I) of the correlation coefficients between the metabolic modules and the microbial modules. In the Sankey plot, the panel showed significant relationships (Spearman p-value < 0.05) between metabolic modules and microbial modules (J). Coloring indicates the direction of association (red: positive; blue: negative)(n=6).

Figure 5. PLS-DA model calculated using amygdaloid collected from the rats (control in blue and PS-NPs-exposed in orange) (A). Heatmap of differential metabolites in amygdaloid (B). Differential metabolites enriched in the pathway classification (C). Scatterplot of significantly enriched KEGG pathways (D). Correlation heatmap and scatter plot of the fecal microbiome(E, F), feces metabolites

(H, I), and amygdaloid metabolites. The correlations between individual omics and phenotypes (G, J). Network analysis showed that dihydrocaffeic-acid was located at the center of the network (K).

Figure 6. The alleviated effects of dihydrocaffeic-acid on the PS-NPs-induced neuroinflammation(TNF-α, IL-6, IL-1β), apoptosis process(Caspase3, BAX, Bcl-2) and abnormal neurotransmitters(5-HT, DA, NE) in the amygdala (A) and serum (B). Volcano plot of differential proteins in the amygdala (C). GO assignment of unigenes in the amygdala transcriptome (D). KEGG assignment of unigenes in the amygdala transcriptome (E). Significant-enriched gene sets identified by gene set enrichment analysis between the control group and PS-NPs group (F). Atp2b2 was identified as the hub gene in the network analysis (G). The gene and protein expressions of the cAMP/PKA/p-CREB/Atp2b2 pathway (H-J).

Declaration of interests

☒ The authors declare that they have no known competing financial interests or personal relationships that could have appeared to influence the work reported in this paper.

☐The authors declare the following financial interests/personal relationships which may be considered as potential competing interests:

Figure 1

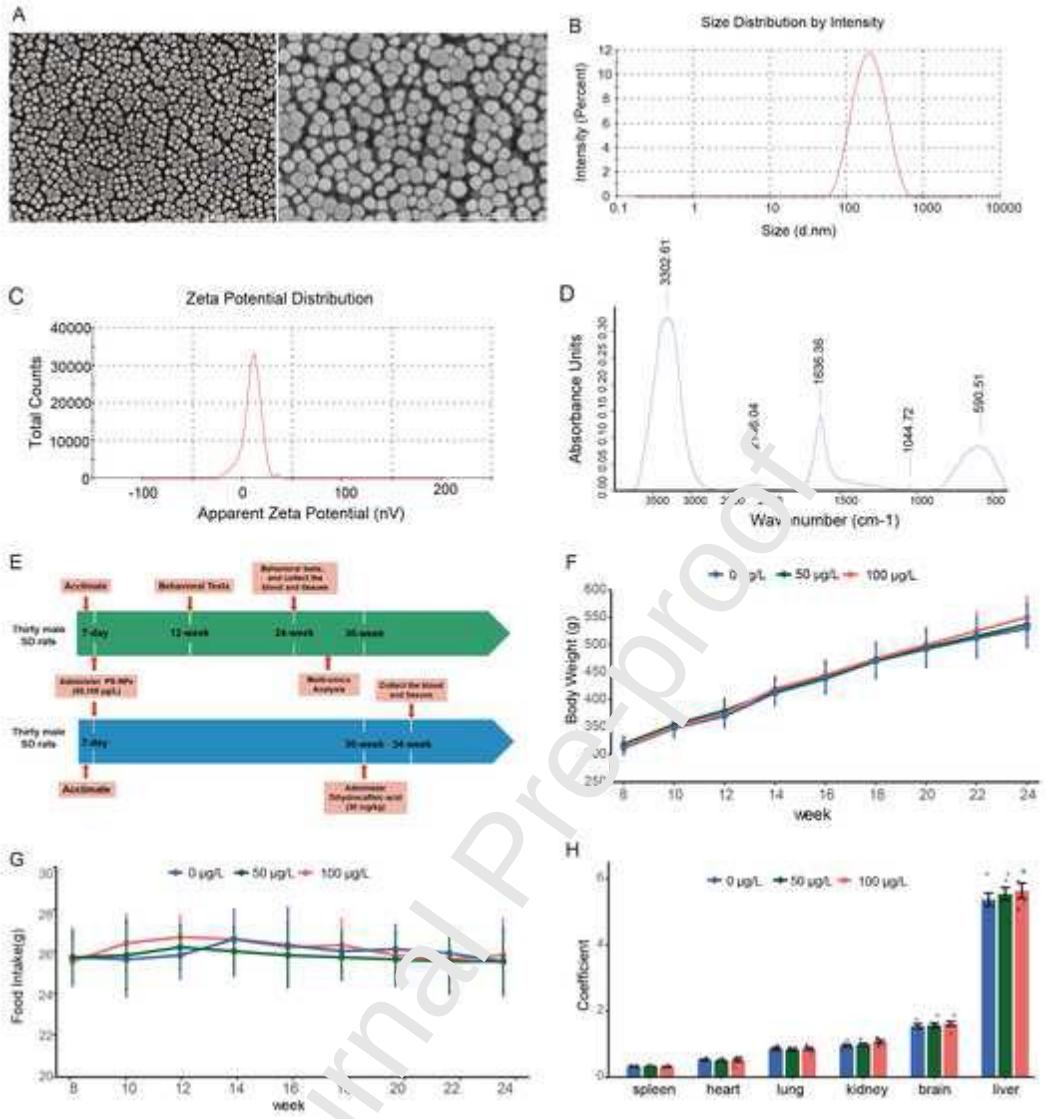

Figure 2

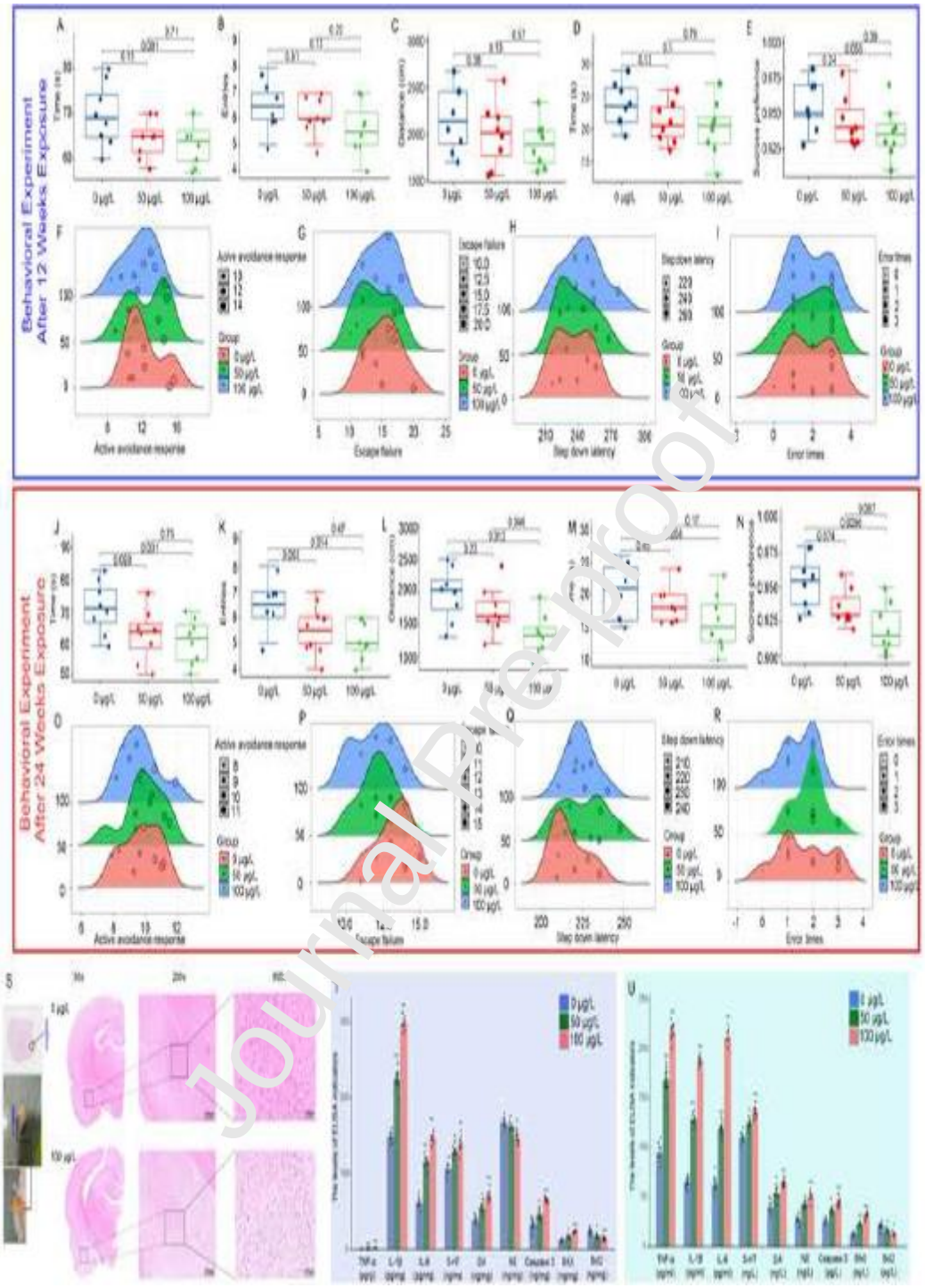

Figure 3

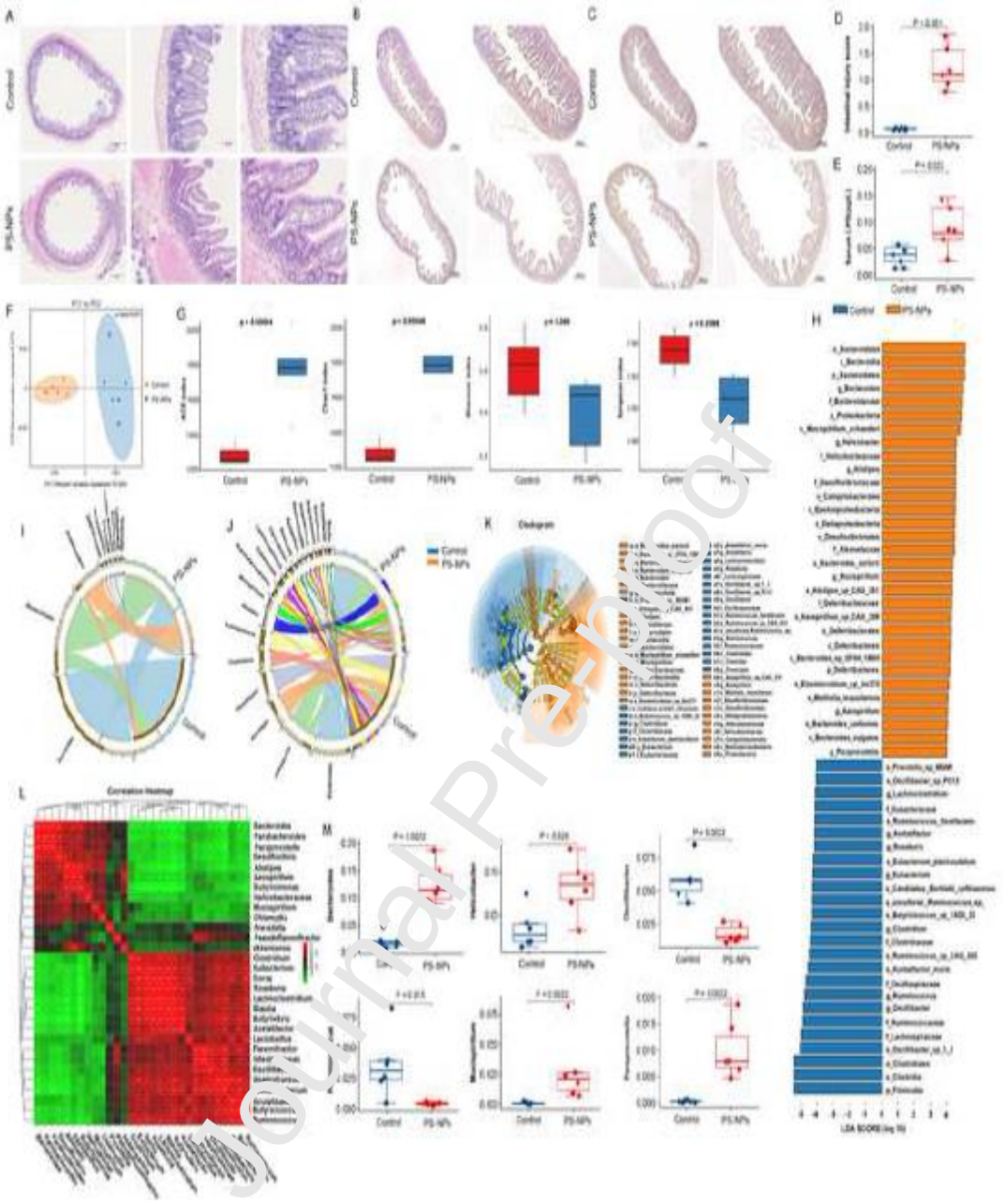

Figure 4

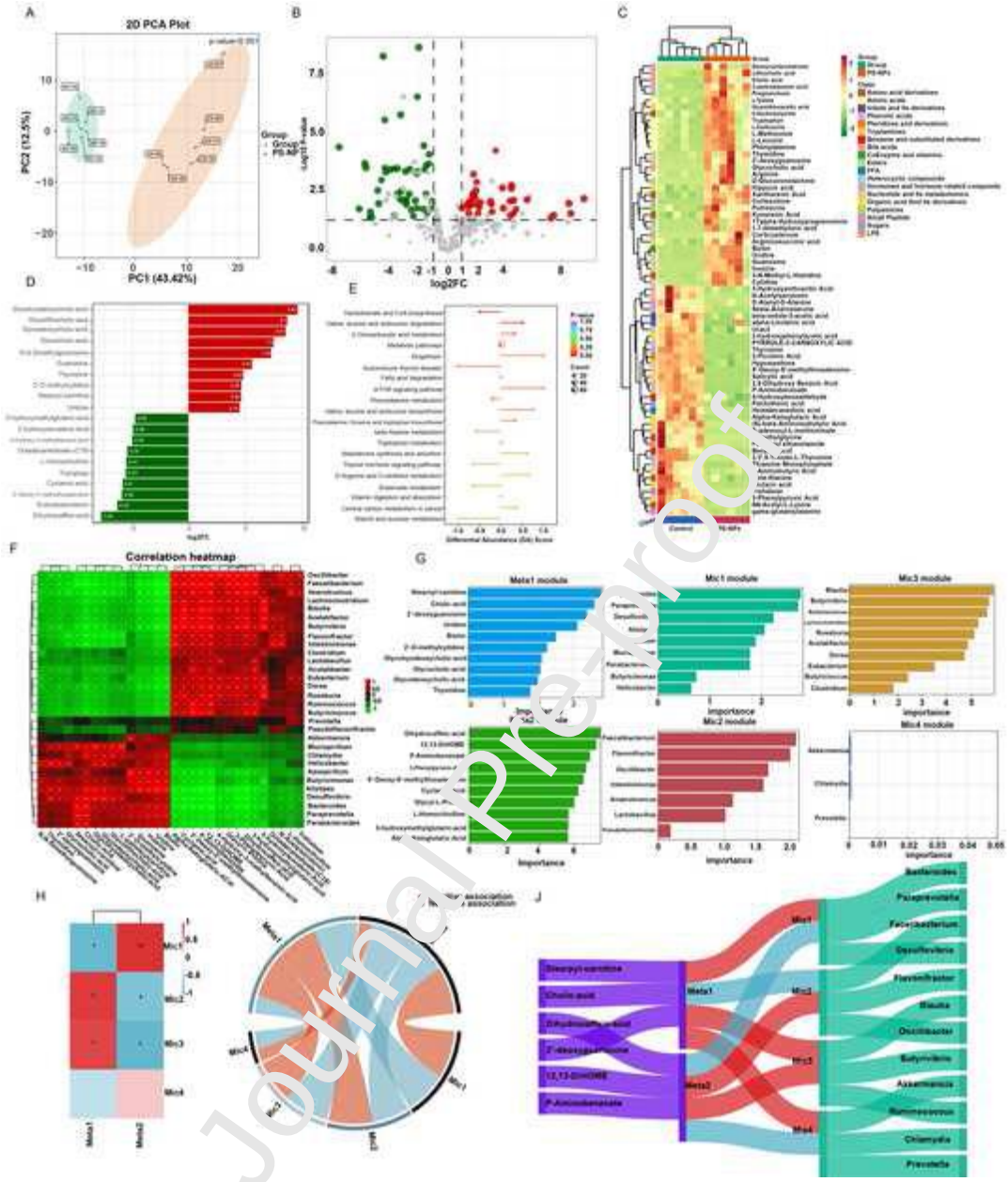

Figure 5

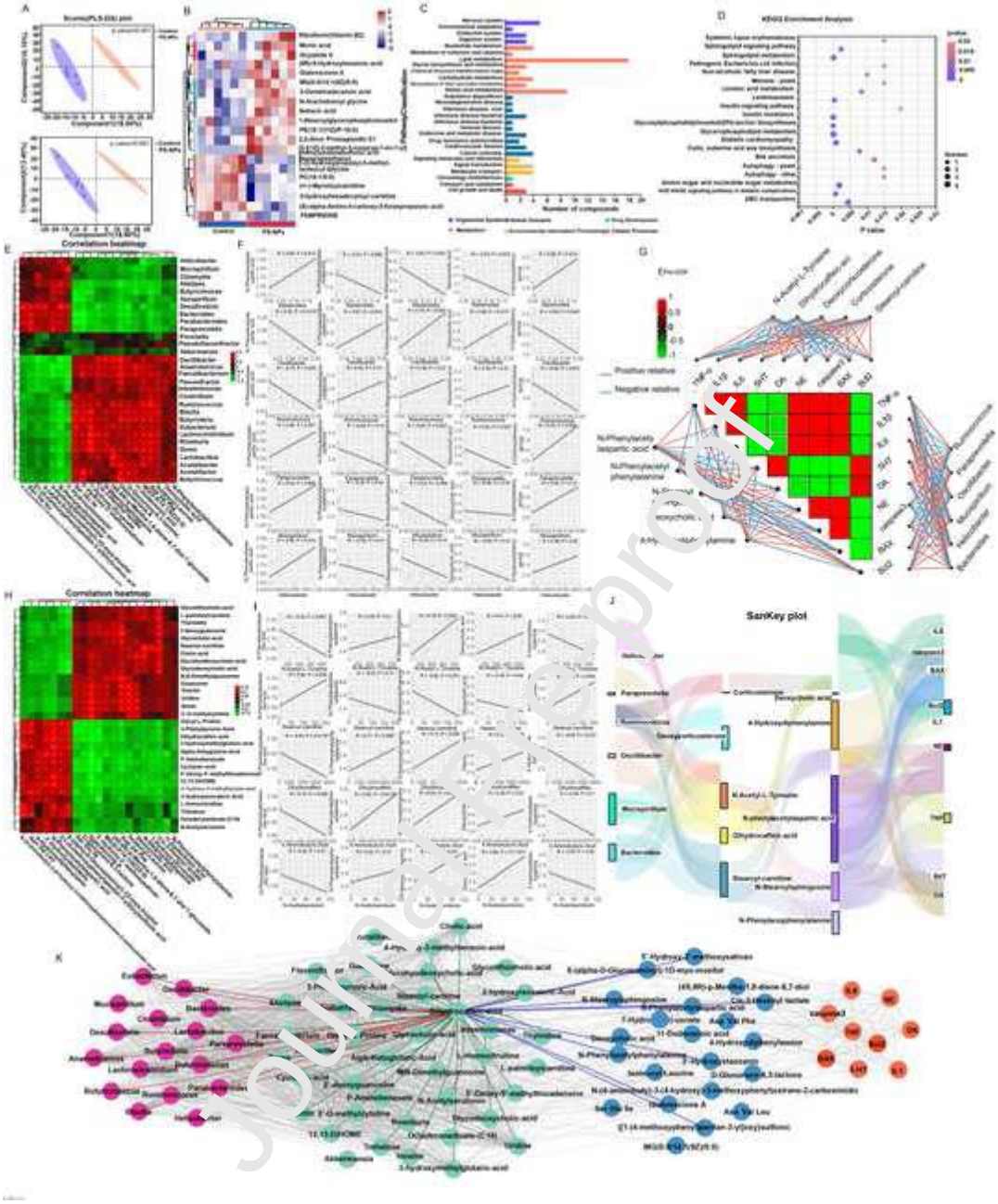

Figure 6

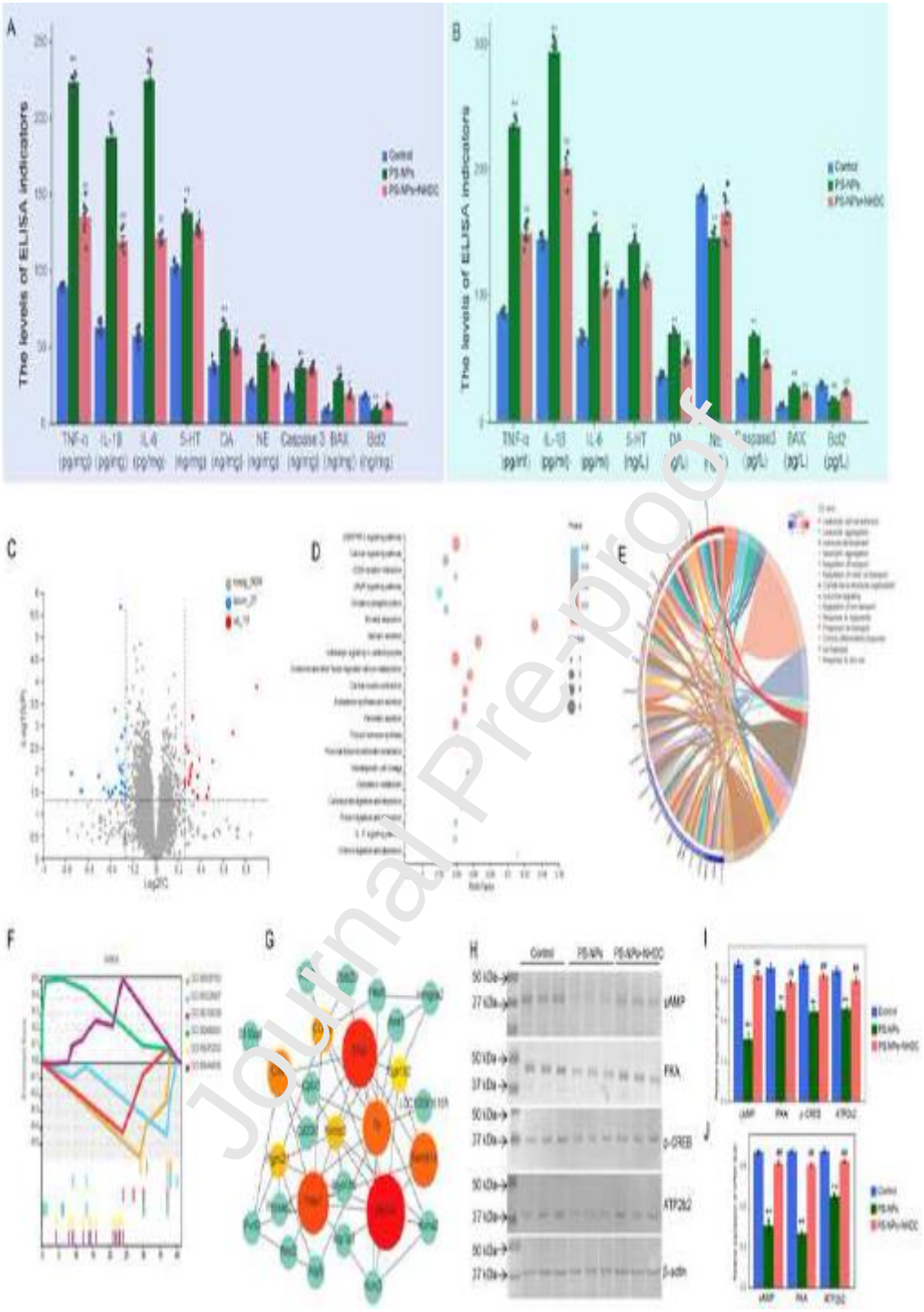

Graphical abstract

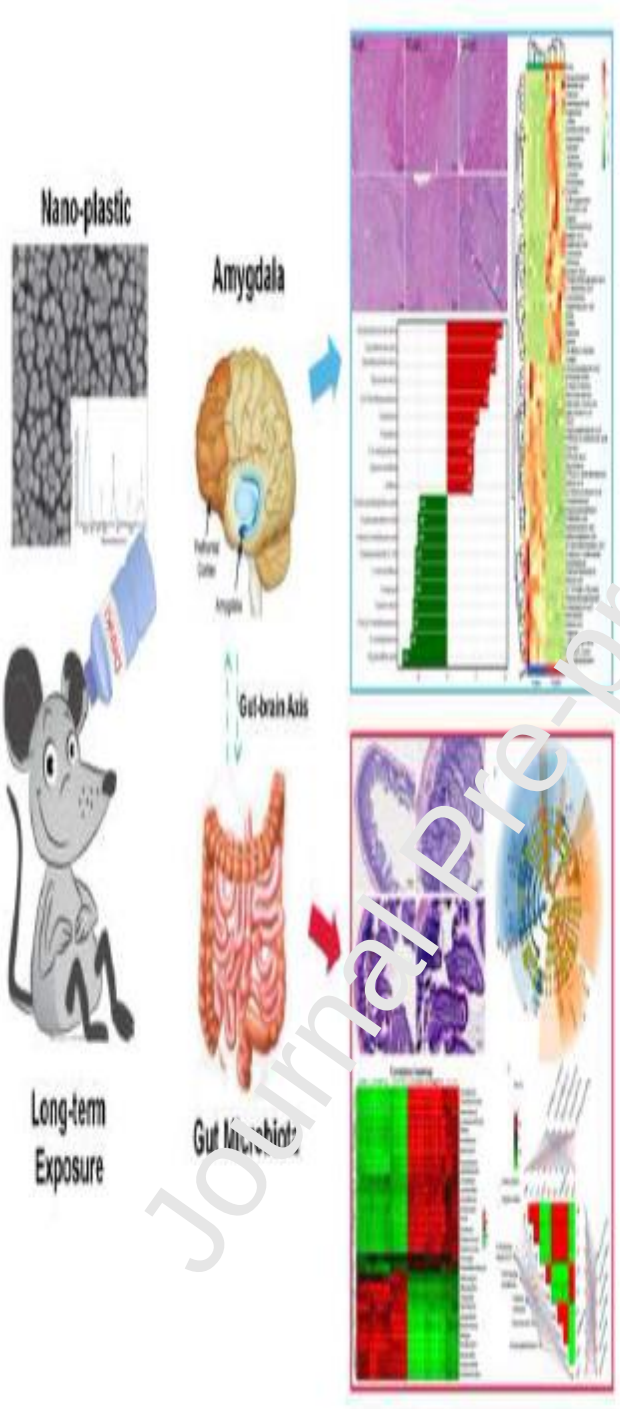

Highlight:

1. Long-term PS-NPs exposure was associated with anxiety-like behavior in rats.
2. PS-NPs exposure could induce aberrant gut microbiome and fecal metabolites.
3. Dihydrocaffeic acid could alleviate PS-NPs-induced adverse effects.